Environmental Science & Technology

Article

pubs.acs.org/est

Fossil Fuel Combustion-Related Emissions Dominate Atmospheric Ammonia Sources during Severe Haze Episodes: Evidence from ^{15}N-Stable Isotope in Size-Resolved Aerosol Ammonium

Yuepeng Pan,[*,†] Shili Tian,[†] Dongwei Liu,[‡] Yunting Fang,[*,‡] Xiaying Zhu,[§] Qiang Zhang,[∥] Bo Zheng,[∥] Greg Michalski,[⊥] and Yuesi Wang[†]

[†]State Key Laboratory of Atmospheric Boundary Layer Physics and Atmospheric Chemistry (LAPC), Institute of Atmospheric Physics, Chinese Academy of Sciences, Beijing 100029, China

[‡]Key Laboratory of Forest Ecology and Management, Institute of Applied Ecology, Chinese Academy of Sciences, Shenyang, Liaoning 110164, China

[§]National Climate Center, China Meteorological Administration, Beijing 100081, China

[∥]Ministry of Education Key Laboratory for Earth System Modeling, Center for Earth System Science, Tsinghua University, Beijing 100084, China

[⊥]Department of Chemistry, Purdue University, 560 Oval Drive, West Lafayette, Indiana 47907, United States

Supporting Information

ABSTRACT: The reduction of ammonia (NH_3) emissions is urgently needed due to its role in aerosol nucleation and growth causing haze formation during its conversion into ammonium (NH_4^+). However, the relative contributions of individual NH_3 sources are unclear, and debate remains over whether agricultural emissions dominate atmospheric NH_3 in urban areas. Based on the chemical and isotopic measurements of size-resolved aerosols in urban Beijing, China, we find that the natural abundance of ^{15}N (expressed using δ^{15}N values) of NH_4^+ in fine particles varies with the development of haze episodes, ranging from −37.1‰ to −21.7‰ during clean/dusty days (relative humidity: ∼ 40%), to −13.1‰ to +5.8‰ during hazy days (relative humidity: 70−90%). After accounting for the isotope exchange between NH_3 gas and aerosol NH_4^+, the δ^{15}N value of the initial NH_3 during hazy days is found to be −14.5‰ to −1.6‰, which indicates fossil fuel-based emissions. These emissions contribute 90% of the total NH_3 during hazy days in urban Beijing. This work demonstrates the analysis of δ^{15}N values of aerosol NH_4^+ to be a promising new tool for partitioning atmospheric NH_3 sources, providing policy makers with insights into NH_3 emissions and secondary aerosols for regulation in urban environments.

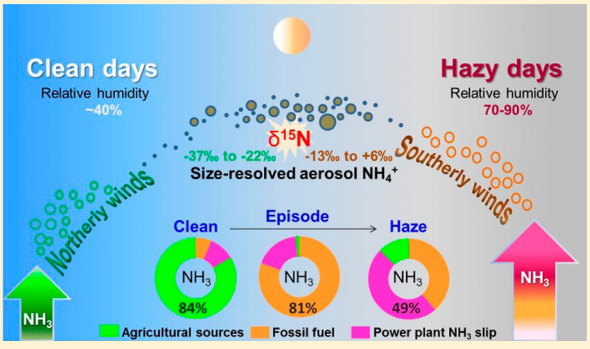

1. INTRODUCTION

Severe and persistent haze episodes in China, which are characterized by extremely high concentrations of particulate matter (PM), are of concern due to regional and global impacts PM has on human health, the environment and climate change.[1,2] The severe PM concentrations in China's urban centers are dominated by secondary aerosols, and their chemical composition is similar to the compositions typically observed in other urban areas.[3] Secondary aerosols can be categorized as either secondary organic aerosols (SOAs) or secondary inorganic aerosols (SIAs), and both of them are important sources of fine (<2.5 μm diameter) particles.[3] In many urban areas of China, such as Beijing, a higher proportion of SIAs relative to SOAs has been observed during haze episodes, suggesting a greater importance of SIAs in haze pollution chemistry.[4] SIAs are mainly formed when the dominant alkaline gas in the lower atmosphere, ammonia (NH_3), reacts with acidic compounds such as sulfuric acid (H_2SO_4) and nitric acid (HNO_3) to form particulate ammonium (NH_4^+).[5] In addition to acid gas to particle conversion, NH_3 can also play a role in aerosol nucleation enhancing SIAs formation and growth by neutralizing H_2SO_4 droplets.[2] However, despite the importance of NH_3 in urban haze chemistry, this pollutant is currently not included in emission control policies in China or in other regions worldwide that also experience severe particulate pollution.[6] Besides, the relative emission strength of individual NH_3 sources remains unclear, and a debate continues over whether NH_3 transported from agricultural regions is the major

Received: February 5, 2016
Revised: June 22, 2016
Accepted: June 30, 2016

DOI: 10.1021/acs.est.6b00634
Environ. Sci. Technol. XXXX, XXX, XXX−XXX

contributor to atmospheric NH_3 in urban areas as opposed to local NH_3 sources. Thus, identifying NH_3 emission sources and quantifying the relative contributions of different sources to the NH_3 budget is important for management strategies designed to reduce the adverse impacts of atmospheric NH_3.[7]

The application of stable nitrogen (N) isotopes as a potential tracer of the origin of NH_3 has been proposed,[7] which might help constrain regional NH_3 budgets. N isotopic signatures in the U.S. revealed that the NH_3 emitted from volatilized livestock waste and fertilizer has relatively low $\delta^{15}N$ values (−56‰ to −23‰, relative to air N_2) that could be used to differentiate it from NH_3 emitted from fossil fuel sources, which have higher $\delta^{15}N$ values (−15‰ to +2‰).[7] This approach was applied in Pittsburgh, an urban center in the U.S., and revealed high $\delta^{15}N$ values (−8.5 ± 7.2‰) of NH_3, which were suggested to mainly originate from fossil fuel combustion-related emissions,[8] despite the fact that global emission inventories indicate that agricultural NH_3 emissions are responsible for 80−93% of NH_3 emissions.[9] To date, atmospheric NH_3 from fossil fuel sources in China has not been accurately quantified, although nonagricultural sources of NH_3 in Beijing have been elucidated during the winter based on correlations between NH_3 and the traffic-related pollutants NO_x and CO.[10,11] In large urban centers, such as Beijing, the high spatial variability of NH_3 concentrations, and the potential complexity of determining NH_3 source attribution in a system with a mixture of multiple sources,[10−12] makes closing the NH_3 budget a challenge. Therefore, quantitative estimates based on the $\delta^{15}N$ technique and other top-down constraints are needed to further quantify the NH_3 sources in large cities.

Here, we present stable N isotopic composition results for NH_4^+ that was sampled using a size-resolved aerosol sampler in urban Beijing during extreme haze episodes in early 2013. These haze pollution events were persistent, and they covered ∼1.3 million km^2 and affected ∼800 million people.[13] PM measurements in urban Beijing showed that the daily average concentrations of PM_{10} and $PM_{2.5}$ exceeded the Chinese National Ambient Air Quality Standard (GB3095−2012, grade I) of 50 and 35 $\mu g\ m^{-3}$ for 88% and 81% of the days, respectively, between January 1 and February 28, 2013, with record-breaking instantaneous concentrations of 995 and 772 $\mu g\ m^{-3}$, respectively, on January 12.[14] Five episodes with mean $PM_{2.5}$ concentrations above 500 $\mu g\ m^{-3}$ occurred in January 2013.[15] These five episodes were cyclic with a period ranging from 4 to 7 days. Such strong haze cycles are regional in nature and are controlled by synoptic scale weather systems, specifically the passage of cold fronts, which induce inversion layers and stagnate air flow.[16] In this study, we focused on the samples collected during the period from January 24 to February 1, which represents an extreme haze pollution episode with a clear periodic cycle of 7 days.

The objective of this study was to identify the major sources of NH_3 in urban regions during haze pollution based on the N isotope fractionation that occurs during the conversion of NH_3 gas to NH_4^+ in fine particles. To our knowledge, this study represents the first isotopic interpretation of size-resolved aerosol NH_4^+ in China and is likely the first such interpretation in a highly urbanized environment in the world. The size-resolved isotopic data collected here are unique and may be useful for characterizing NH_3 sources and N chemistry during haze formation. This information is critical for atmospheric chemistry and transport modeling and for the assessment of haze mitigation policy options in the regions with severe NH_3-related air pollution.

2. MATERIALS AND METHODS

2.1. Aerosol Sampling. The PM sampling was performed on the roof of a building (15 m height) at the State Key Laboratory of Atmospheric Boundary Layer Physics and Atmospheric Chemistry (LAPC), Institute of Atmospheric Physics (IAP), Chinese Academy of Sciences (CAS) in urban Beijing (39°58′ N, 116°22′ E).[12] The site is located in Yuandadu Park and is surrounded by a dense residential area (ca. 7500 persons km^{-2}). The site is approximately 0.8 km north of the third Ring Road and 1.3 km south of the fourth Ring Road, with daily average traffic volumes of approximately 10 million day^{-1} for both ring roads. No major industrial emissions from coal combustion are present in urban Beijing, but residential coal burning during the cold observation period was expected due to home heating.

Size-segregated aerosols were collected using a 9-stage impactor sampler (Anderson Series 20-800) at a flow rate of 28.3 L min^{-1}. The 50% cutoff size bins of the sampler are >9.0, 9.0−5.8, 5.8−4.7, 4.7−3.3, 3.3−2.1, 2.1−1.1, 1.1−0.65, 0.65−0.43, and <0.43 μm. The filter substrate was quartz fiber (Munktell, type MK360, ϕ = 81 mm). Each set of samples was continuously collected for 48 or 24 h, depending on the Air Pollution Prediction Index provided by the local government. Routine sampling was conducted for 48 h from 10:00 (local time) on Monday to 10:00 on Wednesday every week. Intensive sampling intervals of 24 h were also performed to capture the formation and dissipation processes of haze episodes. Procedural aerosol filter blanks were collected for each set of samples and appropriate corrections were applied. In total, 24 sets of size-resolved samples (24 × 9 aerosol filters plus 24 blank filters) were collected during the campaign and subjected to chemical analyses (Supporting Information (SI) Figure S1), and the initial general results have been reported elsewhere.[14]

2.2. Chemical and Isotopic Analysis. Chemical analysis was conducted on a $^1/_4$ section of each quartz filter. Soluble ions in the filter samples were extracted in 25 mL of deionized water (Millipore, 18.2 MΩ) in an ultrasonic bath for 30 min at room temperature. Each extraction solution was passed through a 0.22 μm filter, and the solutes were analyzed using an ion chromatograph (Dionex, ICS-90) for the concentrations of Na^+, NH_4^+, K^+, Mg^{2+}, Ca^{2+}, Cl^-, NO_3^-, and SO_4^{2-}. The mean instrumental limits of detection (LOD) for all the ions were less than 5 $\mu g\ L^{-1}$, and the precision, at 2 mg L^{-1}, was ±5%.

Ten sets of size-resolved samples were selected for N isotopic analysis, which was conducted at the Stable Isotope Ecology Laboratory in the Institute of Applied Ecology, CAS, following the method described by Liu et al.[17] These samples were selected based on the chemical data and the haze development period. In brief, the method is based on the isotopic analysis of nitrous oxide (N_2O). NH_4^+ in the filter extract was initially oxidized to nitrite (NO_2^-) by hypobromite (BrO^-), and NO_2^- was then quantitatively converted into N_2O by hydroxylamine (NH_2OH) under strongly acidic conditions. The produced N_2O was analyzed by a commercially available purge and cryogenic trap system coupled to an isotope ratio mass spectrometer (PT-IRMS, IsoPrime100, IsoPrime Ltd., UK). The $\delta^{15}N$ values are reported in parts per thousand relative to the standard (atmospheric N_2) as follows:

DOI: 10.1021/acs.est.6b00634
Environ. Sci. Technol. XXXX, XXX, XXX−XXX

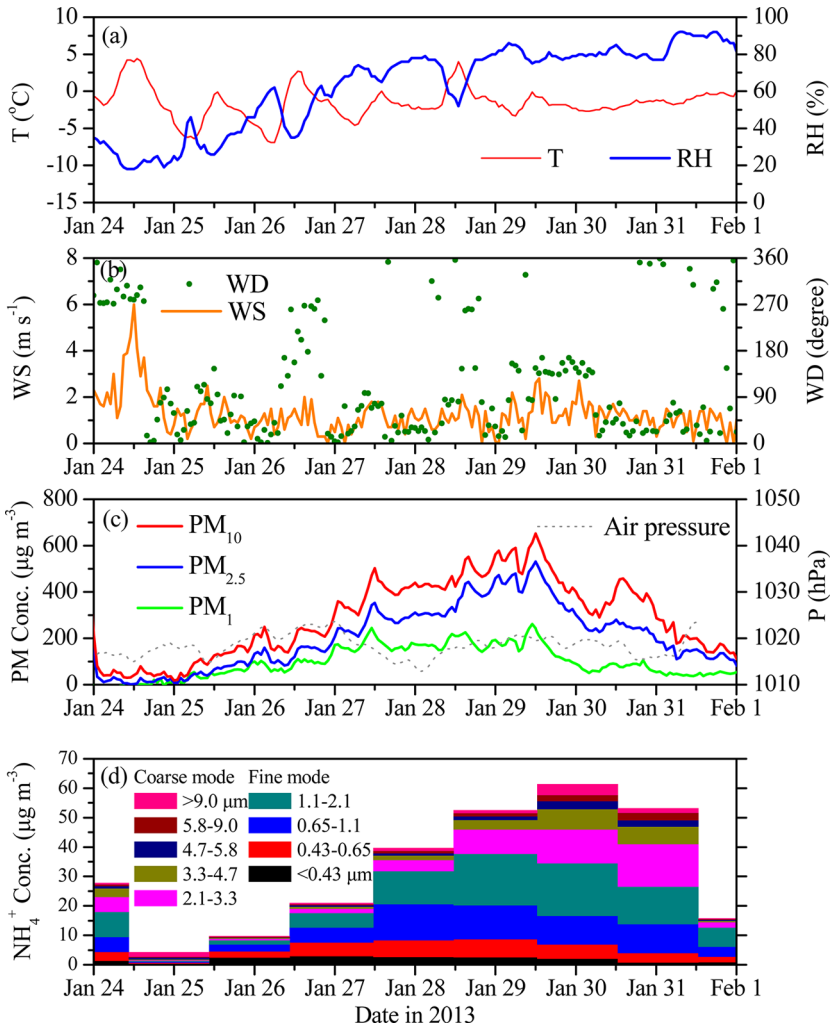

Figure 1. Size-resolved aerosol NH_4^+ concentrations vs particulate matter and meteorological parameters. Meteorological conditions (temperature-T, relative humidity-RH, wind speed-WS and wind direction-WD) were recorded by an automatic meteorological observation instrument (Milos520, Vaisala, Finland). In addition, the mass concentrations of PM_1, $PM_{2.5}$ and PM_{10} were measured through a tapered element oscillating microbalance (TEOM,RP1400, Thermal, USA). The results shown in (a), (b) and (c) were derived from our previous report.[14]

$$\delta^{15}N(‰) = \frac{(^{15}N/^{14}N)_{sample} - (^{15}N/^{14}N)_{standard}}{(^{15}N/^{14}N)_{standard}} \times 1000$$

Three international reference standards (IAEA N1, USGS25 and USGS26) were used for the calibration to air N_2, the accepted international standard for N isotopes. The typical analysis size was 4 mL and produced 60 nmol N_2O, with a $\delta^{15}N$ standard deviation of less than 0.3‰ and often less than 0.1‰ based on replicates (n = 3−5).

2.3. Calculation of the $\delta^{15}N$ Value of NH_3 Gas Based on $\delta^{15}N$ Measurement of Aerosol NH_4^+. The $\delta^{15}N$ value of aerosol NH_4^+ ($\delta^{15}N$-NH_4^+) cannot be directly used to trace NH_3 emissions in haze pollution in Beijing due to isotope exchange equilibrium between NH_3 gas and aqueous NH_4^+ in air. This exchange is written as $^{15}NH_{3(g)} + NH_4^+{}_{(aq)} \leftrightarrow NH_{3(g)} + {}^{15}NH_4^+{}_{(aq)}$, and the experimental isotope enrichment factor,[18] $\varepsilon_{NH_4^+ - NH_3}$ = 33‰, agrees well with that predicted by theory.[19] (see SI text for details).

Briefly, at low NH_3:H_2SO_4 stoichiometric ratios (either ammonium bisulfate or sulfate), the neutralization tends to be unidirectional at the onset and favors the reaction of the lighter isotope. In this case, the isotope effect is likely due to the different diffusion rates of isotopologues at the nonturbulent interface between the atmosphere and the aerosol surface at small distances (μm). For the N isotopologues of NH_3, this enrichment factor is $\sqrt{17/18}$ = 0.972. The formation of a hydrated H_2SO_4 aerosol by SO_2 oxidation and the subsequent diffusion of NH_3 into the new aerosol can readily occur. In such a scenario, the initial $\delta^{15}N$ value of NH_4^+ would be approximately −28‰ relative to the ambient NH_3. This assessment is in good agreement with the results of Heaton et al.,[18] who showed an instantaneous $\delta^{15}N$ value of −20‰ relative to reactant NH_3. When the stoichiometric NH_3:H_2SO_4 ratio is reached or exceeded, isotope exchange equilibrium is rapidly achieved, yielding a difference between the $\delta^{15}N$ value of NH_4^+ and NH_3 of +33‰.

The $\delta^{15}N$-NH_4^+ values will depend not only on whether the system is at equilibrium but also on the pH of the deliquesced aerosols. For example, below a pH of 5, for even extreme tropospheric NH_3 mixing ratios, nearly all of the NH_3 will partition into the aqueous phase thus the $\delta^{15}N$ of NH_4^+ values would reflect the $\delta^{15}N$ values of the NH_3 sources.[20] In contrast, at a pH above 12, almost all of the N will occur as NH_3, and the few NH_4^+ aerosols that exist will be +33‰ relative to the $\delta^{15}N$

DOI: 10.1021/acs.est.6b00634
Environ. Sci. Technol. XXXX, XXX, XXX−XXX

values of the NH_3 sources. This effect can be quantified using an isotopic mass balance in a well-mixed closed system as follows:

$$\delta_{aerosol} = \delta_{gas} + \varepsilon_{aerosol-gas}(1 - f)$$

where δ_{gas} and $\delta_{aerosol}$ are the isotopic composition of the initial atmospheric gas and final ion phase in aerosols, respectively, and f is the fraction of the initial gas converted to the ion phase. Thus, δ_{gas} can be calculated from this equation if $\delta_{aerosol}$ and f are available:

$$\delta_{gas} = \delta_{aerosol} - \varepsilon_{aerosol-gas}(1 - f)$$

To obtain f, the concurrent measurement of NH_4^+ and NH_3 concentrations is needed. Although the daily aerosol NH_4^+ concentrations were observed in the present study, daily observations of NH_3 were unavailable. Thus, the WRF-CMAQ model with newly added heterogeneous reactions was applied to reproduce the heterogeneous chemistry and the meteorological anomaly in January 2013 during regional haze formation. The revised CMAQ with heterogeneous chemistry not only captures the magnitude and temporal variation in NH_4^+,[21] but also reproduces the general variations in NH_3 from clean days to hazy days (SI Figure S2). The simulated concentrations of NH_4^+ and NH_3 were used to calculate f, enabling the evaluation of the initial δ^{15}N-NH_3 values, which were then used to estimate the NH_3 emissions.

2.4. Isotope Mixing Model. The "IsoSources" isotopic mixing model was used to determine the fraction of total NH_3 that could be attributed to different NH_3 emission sources.[22,23] This model iteratively generates source isotopic mixtures with fractions that sum to 1. It compares each calculation against a known δ^{15}N endmember value and retains only those signatures that satisfy the known value within some mass balance tolerance, as defined using a data set of feasible solutions. Although this model can only generate feasible solutions (SI Figure S3; presented here as the average probability), it nevertheless provides a systematic mode of constraining the attribution of N sources in an underdetermined system. We applied a mass-balance tolerance of 0.5‰ to our calculations, which is consistent with the analytical uncertainties in the combined N isotope abundance measurements.

In our case, the calculated mixtures reflected combinations of the δ^{15}N values of three main contributors to NH_3 in the urban environment: agricultural sources, fossil fuel sources (coal combustion and vehicle exhaust) and NH_3 slip from power plants, with mean endmember δ^{15}N values of −39.5‰, −2.95‰ and −12.95‰, respectively. The δ^{15}N values assumed uniform distributions for each source range of δ^{15}N-NH_3 values, as observed in a comprehensive inventory of δ^{15}N-NH_3 values from major emission sources in the U.S.[7]

Fossil fuel-related NH_3 arises from two main sources: as a byproduct of three-way catalytic converters that are part of the exhaust system in most modern automobiles, and NH_3 derived from urea that is used in the selective catalytic reduction (SCR) technology operating in some diesel engines and industrial/power generation plants. NH_3 is derived from air N_2 in the former sources and from commercial urea in the latter, both of which have $\delta^{15}N \sim 0$.[24,25] The process that generates NH_3 from both N sources likely produces NH_3 depleted in δ^{15}N,[7] similar to the depletion found in NO produced by catalytic reduction.[26] The amount of δ^{15}N depletion is expected to depend on the temperature of the catalyst and its reduction efficiency. Thus, the δ^{15}N-NH_3 values from automobiles, diesels, or power plants are unlikely to be significantly different between China and the U.S. as the two countries use similar catalytic technology.

3. RESULTS

3.1. Concentrations and Size Distributions of Aerosol NH_4^+. During the extreme haze episode, distinct temporal variation was apparent in the size-resolved aerosol NH_4^+ concentrations; the PM_1, $PM_{2.5}$ and PM_{10} concentrations; and the corresponding meteorological parameters (Figure 1). This episode was divided into three stages: the initial stage (clean days: January 24−25), the development stage (hazy days: January 25−30) and the dissipation stage (haze days: January 30−February 1).

The NH_4^+ concentrations were low during the initial clean days (January 24−25), at which time the air mass originated from the NW and had a low relative humidity (RH) and high wind speed (WS) (Figures 1 and S4). The size distribution of the NH_4^+ concentrations showed a peak at 4.7−5.8 μm, which may be indicative of soil dust.[27] In addition to a peak at 0.65−2.1 μm, a minor peak at 4.7−5.8 μm was found on the dusty day of February 28, with instantaneous PM_{10} concentrations above 1000 μg m^{-3} (Figures 2 and S1).

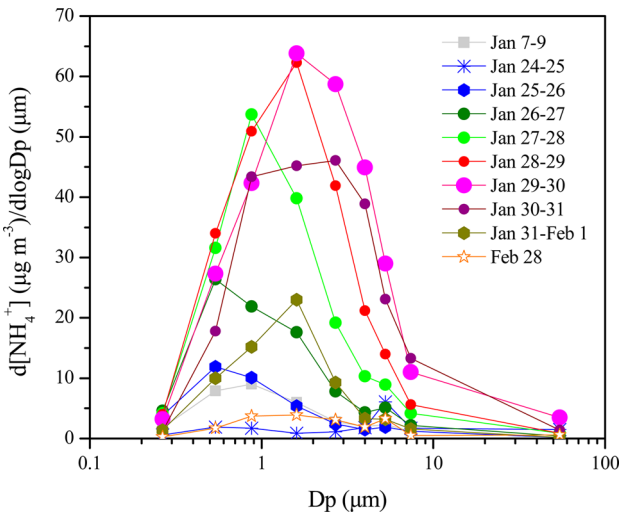

Figure 2. Size distribution of aerosol NH_4^+ during the study period.

During the haze development stage from January 25 to 30, the NH_4^+ concentrations increased significantly from 9.8 to 61.3 μg m^{-3} and preferentially accumulated in the aerosol size bin of 0.65−2.1 μm (Figures 1-2). During this period, the wind was weak, the RH increased from 40% to 90%, and the air masses at heights of 1000−3000 and 100 m were from the NW and SE, respectively (SI Figure S4). Interestingly, the main NH_4^+ particle size shifted from the submicrometer size of 0.43−0.65 μm on January 25−27 to 0.65−1.1 μm on January 27−28 and to 1.1−2.1 μm on January 28−30 (Figure 2). This size shift may have been due to gas-particle conversion and hygroscopic growth with the increase in RH.[14]

During the haze dissipation stage between January 30 and 31, the RH was stable between 80% and 90%, but the NH_4^+ concentrations decreased from 61.3 to 53.1 μg m^{-3} (Figure 1). Unlike the pattern observed during the haze development

DOI: 10.1021/acs.est.6b00634
Environ. Sci. Technol. XXXX, XXX, XXX−XXX

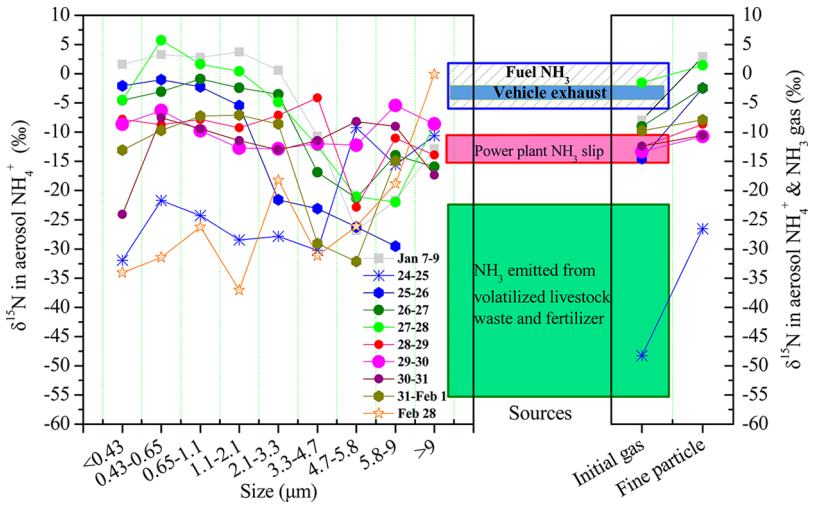

Figure 3. Variations in the $\delta^{15}N$ values of aerosol NH_4^+ with size bins and the initial $\delta^{15}N$-NH_3 values in air against the NH_3 emission signatures of individual sources. The source signatures are obtained from a previous report.[7]

stage, NH_4^+ concentrations decreased in the fine mode (<2.1 μm) but increased in the coarse mode between 2.1 and 4.7 μm during the dissipation stage. This difference in particle NH_4^+ size distribution was likely caused by the enhanced RH that facilitated the hygroscopic growth of coarse particles (>2.1 μm), causing the NH_3 to dissolve on the surface of wet particles. During January 31 to February 1, when the air mass shifted from the SE to the NW with increased WS, the NH_4^+ concentrations decreased to 15.8 $\mu g\ m^{-3}$ and peaked at 1.1−2.1 μm (Figures 1 and 2).

3.2. Isotopic Features of Size-Resolved NH_4^+. Figure 3 plots the $\delta^{15}N$-NH_4^+ values as a function of particle size during the observation period. Since the formation pathway of fine and coarse particles is different, the isotopic features of size-resolved NH_4^+ were discussed separately below.

For fine particles, we observed relatively low $\delta^{15}N$-NH_4^+ values on the clean days of January 24−25, with mean values of −26.6‰ (range: −31.9‰ to −21.7‰). Because the air mass was from the NW during this period, this signature may indicate a regional transport of NH_4^+. This pattern is evident from another dusty day on February 28, with the comparable range of $\delta^{15}N$-NH_4^+ values (−37.1‰ to −26.2‰) found in fine particles. The clean and dusty days are also characterized by low RH (~40%), which could indicate that the particles are less deliquesced; thus the NH_4^+ in transported particles is much slower to equilibrate with local NH_3 sources because it is mostly in the solid phase. In contrast, the increase in RH and NH_4^+ concentrations during the haze development stage suggests that the equilibration of NH_3 with fine particle NH_4^+ became favored under these conditions because the particles are deliquesced and liquid−gas exchange is expected to be rapid. This interpretation is supported by the increase in $\delta^{15}N$-NH_4^+ values from −2.7‰ on January 25−27 and to +1‰ on January 27−28. During the subsequent days, the $\delta^{15}N$-NH_4^+ value was stable at approximately −10‰, although the NH_4^+ concentrations reached their peak on January 29−30 and then decreased from January 30−31 to January 31−February 1.

For coarse particles, the $\delta^{15}N$-NH_4^+ values showed an irregular pattern, which is also different from that of the fine mode. In general, the value of $\delta^{15}N$-NH_4^+ in the coarse mode (except for 2.1−4.7 μm) on January 24−25 was higher than that on January 25−28 but lower than that on January 28-February 1, which is in profound contrast to the temporal pattern of the NH_4^+ concentrations. During the January 28-February 1 period, however, the $\delta^{15}N$-NH_4^+ values in coarse particles (except for 4.7−5.8 μm) tended to increase and showed values similar to those of fine particles.

In addition, the size distribution and isotopic features of NH_4^+ on January 7−9 (hazy days) and February 28 (dusty day) from other pollution episodes exhibited similar patterns to the hazy days and clean days during January 24−February 1 (Figures 2 and 3). Moreover, prior to the arrival at Beijing during the sampling days, the air parcels during this study overlapped with the source regions of NH_4^+ on an annual basis (SI Figure S5). The findings indicate that the results presented are representative and reproducible on a regular basis.

3.3. Tracing NH_3 Emissions Using the Calculated Initial $\delta^{15}N$-NH_3 Values. The $\delta^{15}N$-NH_4^+ values of fine particles observed in this study span a wide range from −37.1‰ to +5.8‰ (Figure 3). This range is similar to that reported at coastal sites, with values of −40‰ to +15‰,[28] but is more depleted than the reported values of 4‰ to +32‰ in marine aerosols.[29] However, these $\delta^{15}N$ values of NH_4^+ may differ from the isotopic composition of the precursor NH_3 due to isotopic fractionation during the conversion from NH_3 gas to aerosol NH_4^+, highlighting the difficulties in tracing the sources of NH_3 using aerosol $\delta^{15}N$-NH_4^+ values. Currently, it is also difficult to perform source apportionment of NH_4^+ in different particle sizes due to the lack of size-resolved isotopic signatures of aerosol NH_4^+. Fortunately, the difference in $\delta^{15}N$-NH_4^+ values among the different size bins in the fine mode was small for a given sampling day, indicating the similarity of their sources. Thus, the concentration-weighted mean of $\delta^{15}N$-NH_4^+ values for fine particles with sizes less than 2.1 μm was used to calculate the initial $\delta^{15}N$-NH_3 values, after accounting for the isotope exchange between NH_3 gas and aerosol NH_4^+.

Figure 3 also shows the calculated results of the initial $\delta^{15}N$-NH_3 value against various NH_3 emission signatures. For clean days, the initial $\delta^{15}N$-NH_3 value was −48‰, which is close to the value of NH_3 from agricultural sources. During the remaining haze days, the initial $\delta^{15}N$-NH_3 value was estimated to be approximately −10‰ (range: −1.6‰ to −14.5‰), which differs from the values of agricultural sources but falls

DOI: 10.1021/acs.est.6b00634
Environ. Sci. Technol. XXXX, XXX, XXX−XXX

within the range of NH_3 related to fossil fuel sources (e.g., vehicles, power plants and coal combustion).[7] This result is the first isotopic evidence showing that fossil fuel combustion, rather than agricultural sources, might be the major source of NH_3 in urban Beijing.

Interestingly, on hazy days, the initial δ^{15}N-NH_3 value fell within the range for vehicle exhaust and power plant slip sources and was comparable to that of aerosol δ^{15}N-NH_4^+ (Figure 3, right). However, on clean days, the difference between aerosol δ^{15}N-NH_4^+ and initial δ^{15}N-NH_3 for the agricultural emissions is substantially larger than that for the other two sources. The lower degree of modification of the original δ^{15}N value of NH_3 gas for these two sources compared with that for agricultural emissions results from the lower gas/aerosol phase distribution of N (hence, higher f) in the air during haze periods. This effect is expected because the concentration of NH_3 is significantly lower than that of NH_4^+ during cold seasons.[11] This is especially true under conditions with lower temperature and higher humidity, which favor the conversion of gaseous NH_3 to particulate NH_4^+.[6] In contrast, NH_3 gas is usually higher than particulate NH_4^+ under warm weather conditions (SI Figure S2-b). In addition, the equilibrium fractionation factor may be greater when temperatures decrease,[30] and this should considered when comparing aerosol δ^{15}N-NH_4^+ values to gas δ^{15}N-NH_3 values under various conditions.

To further quantify the contribution of NH_3 sources to the initial air concentrations of NH_3, the isotope model "IsoSources" was run. The source apportionment results shown in Figure 4 indicate that 84% and 16% of ambient

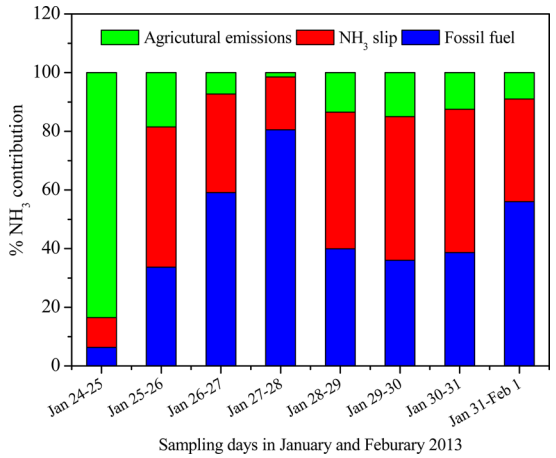

Figure 4. Contributions of individual emissions to the atmospheric concentrations of NH_3 in urban Beijing during the haze episode. Infeasible solutions included days on January 24−25 and January 27−28 when modeled initial isotopic values exceed the maximum or are less than the minimum of the source signature described in sect. 3.3 in this study. Alternatively, the lowest (−56‰) and the highest (+2‰) boundaries of the source signatures summarized for agricultural emissions and fossil fuel combustion were accounted for the aforementioned 2 days, respectively.

NH_3 during the clean days of January 24−25 can be attributed to agricultural emissions and nonagricultural sources, respectively. The reverse was true during hazy days, when nonagricultural sources dominated the ambient NH_3, with a mean contribution of approximately 90%. During the haze development stage, the contribution from fossil fuels increased from 34% (January 25−26) to 59% (January 26−27) and to 81% (January 27−28), whereas the contribution of NH_3 slip (power plants) decreased from 48% (January 25−26) to 34% (January 26−27) and to 18% (January 27−28). However, the percent contributions of fossil fuels and NH_3 slip to each sampling day were comparable during January 28- February 1 (Figure 4). These results suggest that fossil fuel combustion can be a substantial contributor to ambient NH_3 in urban environments during haze pollution, whereas that from agricultural sources can be minor.

4. DISCUSSION

Previous studies showed that the major aerosol compounds, such as nitrate, sulfate, and carbon, in the extreme haze events in early 2013 in China were due to fossil fuel combustion and biomass burning,[1,4,13] but the source of aerosol NH_4^+ was not quantified. This study presents the first isotopic evidence that fossil fuel emissions and NH_3 slip from power plants are more important than agricultural sources during haze pollution periods in urban Beijing. In contrast, agricultural sources are the major sources of NH_3 in the air during clean days when the WS is higher and the air transport is from the SW of Beijing.

The present interpretation is reasonable because agricultural and fossil fuel emissions are usually associated with rural and urban areas, respectively. During haze periods, the atmospheric transport velocity was 50−100 km d^{-1}, as estimated both from the measured surface WS (Figure 1) and by a back-trajectory analysis (SI Figure S4). Under such stagnant weather conditions, local emissions from fossil combustion are expected to be important. In contrast, during clean days, strong winds brought cleaner air from agricultural areas to Beijing. Hence, the ambient NH_3 that formed NH_4^+ aerosols during haze periods in Beijing was sourced at the local, urban scale rather than at the regional scale.

In urban environments, vehicles equipped with three-way catalytic converters can be an important NH_3 source.[31] Previous estimates indicate that in 2005 the total emission of NH_3 from traffic sources was 1.8 kt NH_3−N yr^{-1}, which is half of the amount from agricultural sources in Beijing.[10] The total number of vehicles registered in Beijing, however, has increased by 10% per year, suggesting that the emission of NH_3 by traffic in Beijing during 2013 may have become comparable to that of agricultural emissions.

In addition to being emitted form automobiles, NH_3 is emitted as "fuel NH_3" from electrical generating units (EGUs) and as "NH_3 slip" from EGUs equipped with SCR and selective noncatalytic NO_x reduction (SNCR) technologies.[8] According to a recent report from China's Ministry of Environmental Protection, 25 coal-fired power utilities in Beijing have installed NO_x removal systems. Of these utilities, 16 are controlled through an SCR system (with a total capacity of approximately 3400 MW), and the remaining utilities (with a total capacity of approximately 2000 MW) combine SCR and SNCR. Although it is currently difficult to determine the NH_3 emissions from these sources in Beijing, the emissions are expected to be enormous due to the electricity demand and the fact that extra coal is consumed for residential heating in the winter. A recent finding in Shanghai also highlights the importance of industrial NH_3 emissions, rather than those from vehicles.[6]

The above fossil fuel-based NH_3 emissions are important in urban areas where the abundant acidic compounds (HNO_3 and H_2SO_4) can react with NH_3 to form fine particles, promoting serious haze pollution. Evidence can be found in the positive

DOI: 10.1021/acs.est.6b00634
Environ. Sci. Technol. XXXX, XXX, XXX−XXX

relationship between NH_4^+ and other fossil fuel-related species (SO_4^{2-}, NO_3^-, OC, SO_2, NO_x and CO) in this study (SI Figure S6) and elsewhere.[10,11] Although NH_3 is currently not included in emission control policies in China and is also unregulated in most other regions, the abatement of NH_3 emissions has become an increasing concern to air quality managers, especially during periods of haze pollution.

The results reported here provide the first real isotopic evidence for fossil fuel sources of aerosol NH_4^+ during extreme haze episodes in urban Beijing. The use of stable isotopes of NH_4^+ provides a powerful method to evaluate the relative contribution of fossil fuel-related and agricultural sources, allowing for better targeting of NH_3 reduction. Other nonagricultural area sources of NH_3 emissions include oceans, human waste, vegetation and soils,[32] which are unlikely major contributors during the winter at this location. Additional emissions from biomass/biofuel burning could also contribute, but intense biomass burning was not found based on moderate resolution imaging spectroradiometer (MODIS) fire/hotspot observation (SI Figure S7). We did not include indoor biofuel burning in this study due to the paucity of signature data, a point that should be considered in the interpretation of our results. Other potential limitations in this study include the assumptions that the $\delta^{15}N$ values of the endmembers in China are similar to those in the U.S. and that the parameters used in N fractionation were well constrained. To further reduce the uncertainty in the calculation of initial $\delta^{15}N$-NH_3 values, additional field and laboratory experiments are required to adequately characterize the endmember signatures and the subsequent fractionation process under different air pollution and meteorological conditions.

■ ASSOCIATED CONTENT

Supporting Information

The Supporting Information is available free of charge on the ACS Publications website at DOI: 10.1021/acs.est.6b00634.

Figures S1−S7 illustrate haze pollution events, modeling validation, source apportionment, potential source regions, backward trajectory, various component correlations and fire/hotspot archive, and text details the N fractionation process, with accompanying references (PDF)

■ AUTHOR INFORMATION

Corresponding Authors

*(Y.P.) Phone: +86 01082020530; fax: +86 01062362389; e-mail: panyuepeng@mail.iap.ac.cn.

*(Y.F.) E-mail: fangyt@iae.ac.cn.

Author Contributions

Y.P. and Y.W. conceived and designed the project; Y.P. and S.T. conducted the field work; S.T. and D.L. performed the laboratory experiments; Q.Z. and B.Z. performed the modeling experiments; Y.P., Y.F., X.Z. and G.M. analyzed the data; and Y.P. wrote the paper with comments from the coauthors.

Notes

The authors declare no competing financial interest.

■ ACKNOWLEDGMENTS

This work was supported by the CAS Strategic Priority Research Program (No.: XDA05100100, XDB05020000, and XDB15020200) and the National Natural Science Foundation of China (No.: 31370464, 41405144, 41321064 and 41230642). We are indebted to the staff who collected and analyzed the samples during the study. The authors would like to thank three anonymous reviewers for stimulating a fruitful discussion, due to which some results presented in the original version of the paper could be revised and expanded.

■ REFERENCES

(1) Andersson, A.; Deng, J.; Du, K.; Zheng, M.; Yan, C.; Sköld, M.; Gustafsson, Ö. Regionally-varying combustion sources of the January 2013 severe haze events over eastern China. *Environ. Sci. Technol.* **2015**, *49* (4), 2038−2043.

(2) Zhang, R.; Wang, G.; Guo, S.; Zamora, M. L.; Ying, Q.; Lin, Y.; Wang, W.; Hu, M.; Wang, Y. Formation of urban fine particulate matter. *Chem. Rev.* **2015**, *115* (10), 3803−3855.

(3) Guo, S.; Hu, M.; Zamora, M. L.; Peng, J.; Shang, D.; Zheng, J.; Du, Z.; Wu, Z.; Shao, M.; Zeng, L.; Molinac, M. J.; Zhang, R. Elucidating severe urban haze formation in China. *Proc. Natl. Acad. Sci. U. S. A.* **2014**, *111* (49), 17373−17378.

(4) Sun, Y.; Jiang, Q.; Wang, Z.; Fu, P.; Li, J.; Yang, T.; Yin, Y. Investigation of the sources and evolution processes of severe haze pollution in Beijing in January 2013. *J. Geophys. Res. Atmos.* **2014**, *119* (7), 4380−4398.

(5) Griffith, S. M.; Huang, X. H. H.; Louie, P. K. K.; Yu, J. Z. Characterizing the thermodynamic and chemical composition factors controlling $PM_{2.5}$ nitrate: Insights gained from two years of online measurements in Hong Kong. *Atmos. Environ.* **2015**, *122*, 864−875.

(6) Wang, S.; Nan, J.; Shi, C.; Fu, Q.; Gao, S.; Wang, D.; Cui, H.; Saiz-Lopez, A.; Zhou, B. Atmospheric ammonia and its impacts on regional air quality over the megacity of Shanghai, China. *Sci. Rep.* **2015**, *5*, 15842.

(7) Felix, J. D.; Elliott, E. M.; Gish, T. J.; McConnell, L. L.; Shaw, S. L. Characterizing the isotopic composition of atmospheric ammonia emission sources using passive samplers and a combined oxidation-bacterial denitrifier approach. *Rapid Commun. Mass Spectrom.* **2013**, *27* (20), 2239−2246.

(8) Felix, J. D.; Elliott, E. M.; Gish, T.; Maghirang, R.; Cambal, L.; Clougherty, J. Examining the transport of ammonia emissions across landscapes using nitrogen isotope ratios. *Atmos. Environ.* **2014**, *95*, 563−570.

(9) Reis, S.; Pinder, R. W.; Zhang, M.; Lijie, G.; Sutton, M. A. Reactive nitrogen in atmospheric emission inventories. *Atmos. Chem. Phys.* **2009**, *9* (19), 7657−7677.

(10) Ianniello, A.; Spataro, F.; Esposito, G.; Allegrini, I.; Rantica, E.; Ancora, M. P.; Hu, M.; Zhu, T. Occurrence of gas phase ammonia in the area of Beijing (China). *Atmos. Chem. Phys.* **2010**, *10* (19), 9487−9503.

(11) Meng, Z. Y.; Lin, W. L.; Jiang, X. M.; Yan, P.; Wang, Y.; Zhang, Y. M.; Jia, X. F.; Yu, X. L. Characteristics of atmospheric ammonia over Beijing, China. *Atmos. Chem. Phys.* **2011**, *11* (12), 6139−6151.

(12) Pan, Y.; Wang, Y.; Tang, G.; Wu, D. Wet and dry deposition of atmospheric nitrogen at ten sites in Northern China. *Atmos. Chem. Phys.* **2012**, *12* (14), 6515−6535.

(13) Huang, R.-J.; Zhang, Y.; Bozzetti, C.; Ho, K.-F.; Cao, J.-J.; Han, Y.; Daellenbach, K. R.; Slowik, J. G.; Platt, S. M.; Canonaco, F.; Zotter, P.; Wolf, R.; Pieber, S. M.; Bruns, E. A.; Crippa, M.; Ciarelli, G.; Piazzalunga, A.; Schwikowski, M.; Abbaszade, G.; Schnelle-Kreis, J.; Zimmermann, R.; An, Z.; Szidat, S.; Baltensperger, U.; Haddad, I. E.; Prevot, A. S. H. High secondary aerosol contribution to particulate pollution during haze events in China. *Nature* **2014**, *514* (7521), 218−222.

(14) Tian, S.; Pan, Y.; Liu, Z.; Wen, T.; Wang, Y. Size-resolved aerosol chemical analysis of extreme haze pollution events during early 2013 in urban Beijing, China. *J. Hazard. Mater.* **2014**, *279*, 452−460.

(15) Wang, Y.; Yao, L.; Wang, L.; Liu, Z.; Ji, D.; Tang, G.; Zhang, J.; Sun, Y.; Hu, B.; Xin, J. Mechanism for the formation of the January 2013 heavy haze pollution episode over central and eastern China. *Sci. China: Earth Sci.* **2014**, *57* (1), 14−25.

DOI: 10.1021/acs.est.6b00634
Environ. Sci. Technol. XXXX, XXX, XXX−XXX

(16) Jia, Y.; Rahn, K. A.; He, K.; Wen, T.; Wang, Y., A novel technique for quantifying the regional component of urban aerosol solely from its sawtooth cycles. *J. Geophys. Res.*. **2008**, *113*, (D21), DOI: 10.1029/2008JD010389.
(17) Liu, D.; Fang, Y.; Tu, Y.; Pan, Y. Chemical method for nitrogen isotopic analysis of ammonium at natural abundance. *Anal. Chem.* **2014**, *86* (8), 3787−3792.
(18) Heaton, T. H. E.; Spiro, B.; Robertson, S. M. C. Potential canopy influences on the isotopic composition of nitrogen and sulphur in atmospheric deposition. *Oecologia* **1997**, *109* (4), 600−607.
(19) Urey, H. C. The thermodynamic properties of isotopic substances. *J. Chem. Soc.* **1947**, 562−581.
(20) Seinfeld, J. H.; Pandis, S. N. *Atmospheric Chemistry and Physics: From Air Pollution to Climate Change*, 3rd ed.; John Wiley & Sons: Hoboken, NJ, 2016.
(21) Zheng, B.; Zhang, Q.; Zhang, Y.; He, K. B.; Wang, K.; Zheng, G. J.; Duan, F. K.; Ma, Y. L.; Kimoto, T. Heterogeneous chemistry: a mechanism missing in current models to explain secondary inorganic aerosol formation during the January 2013 haze episode in North China. *Atmos. Chem. Phys.* **2015**, *15* (4), 2031−2049.
(22) Houlton, B. Z.; Sigman, D. M.; Schuur, E. A. G.; Hedin, L. O. A climate-driven switch in plant nitrogen acquisition within tropical forest communities. *Proc. Natl. Acad. Sci. U. S. A.* **2007**, *104* (21), 8902−8906.
(23) Takebayashi, Y.; Koba, K.; Sasaki, Y.; Fang, Y.; Yoh, M. The natural abundance of ^{15}N in plant and soil-available N indicates a shift of main plant N resources to NO_3^- from NH_4^+ along the N leaching gradient. *Rapid Commun. Mass Spectrom.* **2010**, *24* (7), 1001−1008.
(24) Michalski, G.; Kolanowski, M.; Riha, K. M. Oxygen and nitrogen isotopic composition of nitrate in commercial fertilizers, nitric acid, and reagent salts. *Isot. Environ. Health Stud.* **2015**, *51* (3), 382−391.
(25) Bateman, A. S.; Kelly, S. D. Fertilizer nitrogen isotope signatures. *Isot. Environ. Health Stud.* **2007**, *43* (3), 237−247.
(26) Walters, W. W.; Goodwin, S. R.; Michalski, G. Nitrogen stable isotope composition ($\delta^{15}N$) of vehicle-emitted NO_x. *Environ. Sci. Technol.* **2015**, *49* (4), 2278−2285.
(27) Wang, G.; Li, J.; Cheng, C.; Hu, S.; Xie, M.; Gao, S.; Zhou, B.; Dai, W.; Cao, J.; An, Z. Observation of atmospheric aerosols at Mt. Hua and Mt. Tai in central and east China during spring 2009 − Part 1: EC, OC and inorganic ions. *Atmos. Chem. Phys.* **2011**, *11* (9), 4221−4235.
(28) Yeatman, S. G.; Spokes, L. J.; Dennis, P. F.; Jickells, T. D. Comparisons of aerosol nitrogen isotopic composition at two polluted coastal sites. *Atmos. Environ.* **2001**, *35* (7), 1307−1320.
(29) Kundu, S.; Kawamura, K.; Lee, M., Seasonal variation of the concentrations of nitrogenous species and their nitrogen isotopic ratios in aerosols at Gosan, Jeju Island: Implications for atmospheric processing and source changes of aerosols. *J. Geophys. Res.*. **2010**, *115*, (D20), DOI: 10.1029/2009JD013323.
(30) Li, L.; Lollar, B. S.; Li, H.; Wortmann, U. G.; Lacrampe-Couloume, G. Ammonium stability and nitrogen isotope fractionations for NH_4^+−$NH_{3(aq)}$−$NH_{3(gas)}$ systems at 20−70 °C and pH of 2−13: Applications to habitability and nitrogen cycling in low-temperature hydrothermal systems. *Geochim. Cosmochim. Acta* **2012**, *84*, 280−296.
(31) Cape, J. N.; Tang, Y. S.; van Dijk, N.; Love, L.; Sutton, M. A.; Palmer, S. C. F. Concentrations of ammonia and nitrogen dioxide at roadside verges, and their contribution to nitrogen deposition. *Environ. Pollut.* **2004**, *132* (3), 469−478.
(32) Galloway, J. N.; Dentener, F. J.; Capone, D. G.; Boyer, E. W.; Howarth, R. W.; Seitzinger, S. P.; Asner, G. P.; Cleveland, C. C.; Green, P. A.; Holland, E. A.; Karl, D. M.; Michaels, A. F.; Porter, J. H.; Townsend, A. R.; Vöosmarty, C. J. Nitrogen Cycles: Past, Present, and Future. *Biogeochemistry* **2004**, *70* (2), 153−226.

DOI: 10.1021/acs.est.6b00634
Environ. Sci. Technol. XXXX, XXX, XXX−XXX